

Oxy-schorl, $\text{Na}(\text{Fe}_2^+\text{Al})\text{Al}_6\text{Si}_6\text{O}_{18}(\text{BO}_3)_3(\text{OH})_3\text{O}$, a new mineral from Zlatá Idka, Slovak Republic and Příbyslavice, Czech Republic

PETER BAČÍK,^{1,*} JAN CEMPÍREK,^{2,3} PAVEL UHER,¹ MILAN NOVÁK,⁴ DANIEL OZDÍN,¹ JAN FILIP,⁵ RADEK ŠKODA,⁴ KAREL BREITER,⁶ MARIANA KLEMENTOVÁ,⁷ RUDOLF ĎUŠA,⁸ AND LEE A. GROAT³

¹Department of Mineralogy and Petrology, Comenius University, Mlynská dolina, 842 15 Bratislava, Slovakia

²Department of Mineralogy and Petrography, Moravian Museum, Zelný trh 6, 659 37 Brno, Czech Republic

³Department of Earth, Ocean, and Atmospheric Sciences, University of British Columbia, 6339 Stores Road, Vancouver, British Columbia V6T 164, Canada

⁴Department of Geological Sciences, Masaryk University, Kotlářská 2, 611 37 Brno, Czech Republic

⁵Regional Centre of Advanced Technologies and Materials, Palacký University in Olomouc, 17. listopadu 12, 771 46 Olomouc, Czech Republic

⁶Geological Institute of the Academy of Science of Czech Republic, v.v.i., Rozvojová 269, 165 00 Praha 6, Czech Republic

⁷Institute of Physics of the AS CR, v.v.i., Na Slovance 2, 182 21 Praha 8, Czech Republic

⁸Bystrická 87, 040 11 Košice, Slovakia

ABSTRACT

Oxy-schorl (IMA 2011-011), ideally $\text{Na}(\text{Fe}_2^+\text{Al})\text{Al}_6\text{Si}_6\text{O}_{18}(\text{BO}_3)_3(\text{OH})_3\text{O}$, a new mineral species of the tourmaline supergroup, is described. In Zlatá Idka, Slovak Republic (type locality), fan-shaped aggregates of greenish black acicular crystals ranging up to 2 cm in size, forming aggregates up to 3.5 cm thick were found in extensively metasomatically altered metarhyolite pyroclastics with Qtz+Ab+Ms. In Příbyslavice, Czech Republic (co-type locality), abundant brownish black subhedral, columnar crystals of oxy-schorl, up to 1 cm in size, arranged in thin layers, or irregular clusters up to 5 cm in diameter, occur in a foliated muscovite-tourmaline orthogneiss associated with Kfs+Ab+Qtz+Ms+Bt+Grt. Oxy-schorl from both localities has a Mohs hardness of 7 with no observable cleavage and parting. The measured and calculated densities are 3.17(2) and 3.208 g/cm³ (Zlatá Idka) and 3.19(1) and 3.198 g/cm³ (Příbyslavice), respectively. In plane-polarized light, oxy-schorl is pleochroic; *O* = green to bluish-green, *E* = pale yellowish to nearly colorless (Zlatá Idka) and *O* = dark grayish-green, *E* = pale brown (Příbyslavice), uniaxial negative, $\omega = 1.663(2)$, $\epsilon = 1.641(2)$ (Zlatá Idka) and $\omega = 1.662(2)$, $\epsilon = 1.637(2)$ (Příbyslavice). Oxy-schorl is trigonal, space group *R3m*, *Z* = 3, *a* = 15.916(3) Å, *c* = 7.107(1) Å, *V* = 1559.1(4) Å³ (Zlatá Idka) and *a* = 15.985(1) Å, *c* = 7.154(1) Å, *V* = 1583.1(2) Å³ (Příbyslavice). The composition (average of 5 electron microprobe analyses from Zlatá Idka and 5 from Příbyslavice) is (in wt%): SiO₂ 33.85 (34.57), TiO₂ <0.05 (0.72), Al₂O₃ 39.08 (33.55), Fe₂O₃ not determined (0.61), FeO 11.59 (13.07), MnO <0.06 (0.10), MgO 0.04 (0.74), CaO 0.30 (0.09), Na₂O 1.67 (1.76), K₂O <0.02 (0.03), F 0.26 (0.56), Cl 0.01 (<0.01), B₂O₃ (calc.) 10.39 (10.11), H₂O (from the crystal-structure refinement) 2.92 (2.72), sum 99.29 (98.41) for Zlatá Idka and Příbyslavice (in parentheses). A combination of EMPA, Mössbauer spectroscopy, and crystal-structure refinement yields empirical formulas $(\text{Na}_{0.591}\text{Ca}_{0.103}\square_{0.306})_{\Sigma 1.000}(\text{Al}_{1.885}\text{Fe}_{1.108}\text{Mn}_{0.005}\text{Ti}_{0.002})_{\Sigma 3.000}(\text{Al}_{5.428}\text{Mg}_{0.572})_{\Sigma 6.000}(\text{Si}_{5.506}\text{Al}_{0.494})_{\Sigma 6.000}\text{O}_{18}(\text{BO}_3)_3(\text{OH})_3(\text{O}_{0.625}\text{OH}_{0.236}\text{F}_{0.136}\text{Cl}_{0.003})_{\Sigma 1.000}$ for Zlatá Idka, and $(\text{Na}_{0.586}\text{Ca}_{0.017}\text{K}_{0.006}\square_{0.391})_{\Sigma 1.000}(\text{Fe}_{1.879}\text{Mn}_{0.015}\text{Al}_{1.013}\text{Ti}_{0.093})_{\Sigma 3.000}(\text{Al}_{5.732}\text{Mg}_{0.190}\text{Fe}_{0.078})_{\Sigma 6.000}(\text{Si}_{5.944}\text{Al}_{0.056})_{\Sigma 6.000}\text{O}_{18}(\text{BO}_3)_3(\text{OH})_3(\text{O}_{0.579}\text{F}_{0.307}\text{OH}_{0.115})_{\Sigma 1.000}$ for Příbyslavice. Oxy-schorl is derived from schorl end-member by the $\text{AlOFe}_{-1}(\text{OH})_{-1}$ substitution. The studied crystals of oxy-schorl represent two distinct ordering mechanisms: disorder of R²⁺ and R³⁺ cations in octahedral sites and all O ordered in the *W* site (Zlatá Idka), and R²⁺ and R³⁺ cations ordered in the *Y* and *Z* sites and O disordered in the *V* and *W* sites (Příbyslavice).

Keywords: Oxy-schorl, tourmaline-supergroup minerals, new mineral, electron microanalysis, crystal-structure refinement, Příbyslavice, Zlatá Idka

INTRODUCTION

Minerals of the tourmaline-supergroup are common in many geological environments. The complexity of their structure, including a variability of structural sites and chemical composition are manifested in a relatively large number of mineral species (Henry et al. 2011). Oxy-schorl, ideally $\text{Na}(\text{Fe}_2^+\text{Al})\text{Al}_6\text{Si}_6\text{O}_{18}(\text{BO}_3)_3(\text{OH})_3\text{O}$, is a new member of the

alkali group and oxy-series of the tourmaline supergroup (sensu nomenclature of Henry et al. 2011). The coupled general substitution ${}^Y\text{R}^{2+}+{}^W(\text{OH}) \leftrightarrow {}^Y\text{Al}+{}^W\text{O}$ derived from ideal schorl $\text{NaFe}_2^+\text{Al}_6\text{Si}_6\text{O}_{18}(\text{BO}_3)_3(\text{OH})_3\text{O}$ and leading to the ideal oxy-schorl was discussed already by Foit and Rosenberg (1977). Povondra (1981), Povondra et al. (1985, 1987), and Foit (1989) published several chemical analyses of tourmalines corresponding to oxy-schorl including samples from the co-type locality Příbyslavice (Povondra et al. 1987). However, the term oxy-schorl was first introduced by Hawthorne and Henry (1999).

* E-mail: bacikp@fns.uniba.sk

Subsequently, oxy-schorl was described from several localities worldwide (e.g., Henry and Dutrow 2001; Novák et al. 2004; Baksheev et al. 2011). Finally, oxy-schorl was defined as a potential new species of the tourmaline supergroup in the recent tourmaline nomenclature (Henry et al. 2011). Oxy-schorl is likely quite a common mineral species; however, many tourmaline compositions are close to the simplified formula $(\text{Na}_{0.5}\square_{0.5})\text{Fe}_2^+\text{AlAl}_6\text{Si}_6\text{O}_{18}(\text{BO}_3)_3(\text{OH})_3(\text{OH}_{0.5}\text{O}_{0.5})$ (see e.g., Povondra 1981; Foit 1989; Novák et al. 2004) and owing to problems with the determination of H (and other light elements), the exact classification of such schorlitic tourmalines is complicated.

Oxy-schorl was approved by the Commission on New Minerals, Nomenclature and Classification of the International Mineralogical Association under the number IMA 2011-011. The holotype material from the type locality (Zlatá Idka, Slovak Republic) is preserved in the collection of the East-Slovak Museum, Košice, Slovakia (specimen number G-12760), and in the collection of Department of Mineralogy and Petrology, Comenius University, Bratislava, Slovakia (specimen number 7279). Oxy-schorl from co-type locality (Přibyslavice, Czech Republic) is deposited in the collections of the Department of Mineralogy and Petrography, Moravian Museum, Brno, Czech Republic, specimen number B10521. We provide here a description of the physical, chemical, and structural characteristics of oxy-schorl as a new mineral species.

OCCURRENCE AND PHYSICAL PROPERTIES

Oxy-schorl was found in fracture fillings cutting altered metarhyolite pyroclastics, in the abandoned Marianna adit, ca. 2.5 km WNW from Zlatá Idka village (48°46'7"N, 20°57'50"E), Slovak Ore Mountains (Slovenské Rudohorie), near Košice, eastern Slovakia. The acid metapyroclastic rocks of Middle Ordovician age belong to the Bystrý Potok Formation of the Gelnica Group, Gemeric Superunit, Central Western Carpathians (Vozárová et al. 2010). Associated minerals of the host-rock include quartz, albite, and muscovite. Oxy-schorl is probably a product of the interaction between the metarhyolite pyroclastics and boron-enriched, hydrothermal fluids generated from adjacent Permian tourmaline-bearing leucogranites. Oxy-schorl from Zlatá Idka occurs in fan-shaped aggregates of greenish black acicular crystals ranging up to 2 cm in size, with aggregates up to 3.5 cm across. Tourmaline aggregates display chemical zoning in backscattered electron (BSE) images (Fig. 1), locally with a more Mg-rich (dravite to oxy-dravite) and also *X*-site vacant composition ("□-Fe-O root name" according to Henry et al. 2011) but the oxy-schorl composition prevails.

The second occurrence of oxy-schorl is in a foliated muscovite-tourmaline orthogneiss at Přibyslavice (Tisá skála outcrop, ~1 km ENE from Přibyslavice, 49°50'48"N, 15°25'1"E) near Kutná Hora, Central Bohemia Region, Czech Republic. The host, lower palaeozoic muscovite-tourmaline alkali-feldspar granite was metamorphosed during the Variscan orogeny in the amphibolite facies (Breiter et al. 2010). The orthogneiss is composed of K-feldspar (orthoclase perthite), albite, quartz, muscovite, biotite, garnet, and apatite with accessory zircon, magnetite, pyrite, and ilmenite. Oxy-schorl from Přibyslavice formed as a primary magmatic mineral of the granite, but its composition was influenced by the later metamorphic processes

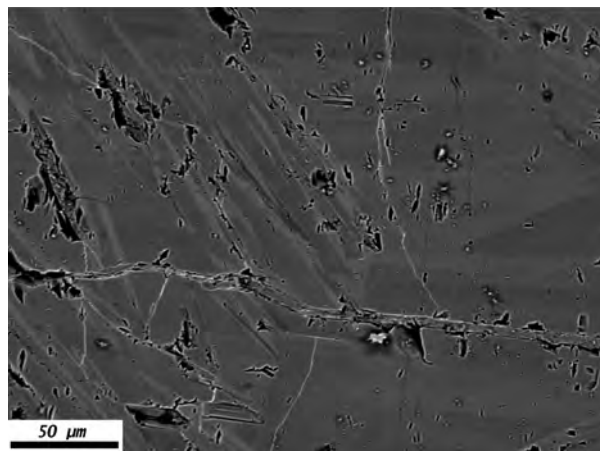


FIGURE 1. BSE image of oxy-schorl from Zlatá Idka. The zoning is given by the variation in Fe, Mg, and Al content; dark-gray zone corresponds to transitional oxy-schorl to "□-Fe-O root name" tourmaline composition.

(e.g., Povondra et al. 1987, 1998). It forms abundant subhedral, columnar homogeneous crystals, up to 1 cm in size, arranged in thin layers, or irregular clusters up to 5 cm in diameter.

Oxy-schorl from both localities has a vitreous luster and is translucent in thin edges, non-fluorescent and paramagnetic. Its Mohs hardness is 7, it is brittle and has conchoidal fracture; cleavage and parting were not observed. The streak is pale gray. The density was measured using a pycnometric method as 3.17(2) and 3.19(1) g/cm³; calculated density using empirical formula and unit-cell data yields 3.208 and 3.198 g/cm³ for oxy-schorl from Zlatá Idka and Přibyslavice, respectively. Oxy-schorl is negative uniaxial with the following optical properties: $\omega = 1.663(2)$, $\epsilon = 1.641(2)$, birefringence: 0.022 (589.9 nm) in Zlatá Idka and $\omega = 1.662(2)$; $\epsilon = 1.637(2)$; birefringence: 0.025 (589.9 nm) in Přibyslavice. At both localities, oxy-schorl has distinct pleochroism; *O* = green to bluish-green, *E* = pale yellowish to nearly colorless (Zlatá Idka) and *O* = dark grayish-green, *E* = pale brown (Přibyslavice).

ANALYTICAL METHODS

Chemical composition

Representative chemical analyses (5 from Zlatá Idka, 5 from Přibyslavice) were carried out using a CAMECA SX100 electron microprobe (WDS mode, 15 kV, 10 and 20 nA, 5 μm beam diameter) on the same crystals used for structure refinement. The following standards were used: almandine (SiK α , FeK α), titanite (TiK α), sanidine (AlK α , KK α), chromite (CrK α), vanadinite (VK α), spessartine (MnK α), MgO (MgK α), grossular (CaK α), albite (NaK α), topaz (FK α), and NaCl (ClK α). Detection limits of the measured elements vary between 0.01 and 0.05 wt%. Formulas of tourmalines were calculated on a basis of 15 Y+Z+T cations. H₂O was calculated on the basis of an electroneutral formula and structure refinement results. The presence of H₂O was confirmed by IR spectroscopy. B₂O₃ was calculated from ideal formulas since the structure refinement data indicate full occupancy of the *B* site and absence of ¹¹B in the *T* site. Ti and Cl were below detection limits (0.05 and 0.01 wt%, respectively). Analytical data are given in Table 1. The content of Li in oxy-schorl from Zlatá Idka was determined by LA-ICP-MS analysis with a laser ablation system UP 213 (New Wave, U.S.A.) and quadrupole ICP-MS spectrometer Agilent 7500 CE (Agilent, Japan), at the Central European Institute of Technology, Masaryk University, Brno. It was always lower than the detection limit, which corresponded to 0.04 wt% Li₂O. Oxy-schorl from Přibyslavice yielded Li₂O \leq 0.06 wt% determined by wet chemical analysis (Povondra et al. 1987).

TABLE 1. Chemical composition and formula of oxy-schorl from Zlatá Idka and Příbyslavice

Zlatá Idka				Příbyslavice			
SiO ₂ wt%	33.10	Si apfu	5.506	SiO ₂ wt%	34.57	Si apfu	5.944
TiO ₂	0.02	^z Al	0.494	TiO ₂	0.72	^z Al	0.056
B ₂ O ₃ *	10.45	Sum T	6.000	B ₂ O ₃ *	10.11	Sum T	6.000
Al ₂ O ₃	39.81			Al ₂ O ₃	33.55		
FeO	7.97	B	3.000	Fe ₂ O ₃	0.61	B	3.000
MgO	2.31			FeO	13.07		
MnO	0.03	^z Al	5.428	MnO	0.10	^z Al	5.732
CaO	0.58	^z Mg	0.572	MgO	0.74	^z Mg	0.190
Na ₂ O	1.83	Sum Z	6.000	CaO	0.09	Fe ³⁺	0.078
F	0.26			K ₂ O	0.03	Sum Z	6.000
Cl	0.01	Ti	0.002	Na ₂ O	1.76		
H ₂ O†	2.92	^y Al	1.885	Cl	0.00	^y Al	1.013
O=F	0.11	Fe ²⁺	1.108	F	0.56	Ti ⁴⁺	0.093
Total	99.18	Mn	0.005	H ₂ O†	2.72	Fe ²⁺	1.879
		Sum Y	3.000	-O=F,Cl	-0.24	Mn ²⁺	0.015
				Total	98.39	Sum Y	3.000
		Ca	0.103				
		Na	0.591			Ca	0.017
		□	0.306			Na	0.586
		Sum X	1.000			K	0.006
						□	0.391
		^y OH	3.000			Sum X	1.000
		^w OH	0.236			^y OH	3.000
		F	0.136				
		Cl	0.003			^w OH	0.115
		O	0.625			O	0.579
		Sum W	1.000			F	0.307

* Calculated by structural refinement

† Calculated on the basis of electroneutral formula and structure refinement results.

TABLE 2. Hyperfine parameters (Mössbauer spectroscopy) of oxy-schorl

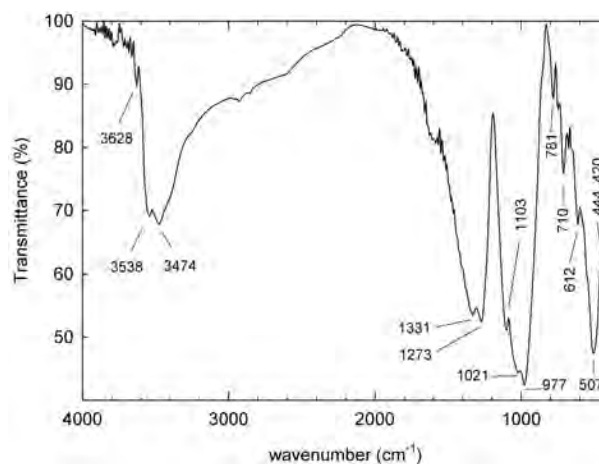
	Isomer shift (mm/s)	Quadrupole splitting (mm/s)	Assignment	Relative abundance (%)
Zlatá Idka	0.98	2.45	^y Fe ²⁺	43
	0.98	2.13	^z Fe ²⁺	13
	0.98	1.64	^z Fe ²⁺	44
Příbyslavice	1.09	2.47	^y Fe ²⁺	37
	1.08	2.15	^z Fe ²⁺	35
	1.04	1.58	^z Fe ²⁺	25
	0.37	0.32	^y Fe ³⁺	4

Mössbauer spectroscopy

The ⁵⁷Fe Mössbauer spectrum of powdered tourmaline (ground under acetone using an agate mortar) was acquired at constant acceleration mode using a ⁵⁷Co in Rh source at room temperature (293 K), at the Department of Nuclear Physics, Slovak Technical University, Bratislava, Slovakia (Zlatá Idka) and Centre for Nanomaterial Research, Faculty of Science, Palacký University in Olomouc (Příbyslavice). The isomer shift was calibrated against an α-Fe foil at room temperature. Spectra were fitted by Lorentz functions using the NORMOS program¹ on the Zlatá Idka sample and CONFIT2000 program (Žák and Jirásková 2006) on the Příbyslavice sample. The fitting results are listed in Table 2.

Infrared spectroscopy

The FTIR spectrum of tourmaline from Příbyslavice was recorded using a Nicolet Nexus 670 spectrometer equipped with DTGS detector and XT-KBr beamsplitter. The sample was prepared by mixing 1 mg of powdered sample with 300 mg of KBr (dried beforehand at 150 °C) and pressing in an evacuated die at 10 tons. A total of 32 scans in air were carried out for the sample in the wavenumber range 4000–400 cm⁻¹ at a resolution of 4 cm⁻¹. The spectrum is shown in Figure 2, and a basic interpretation of the peaks (after Reddy et al. 2007) is listed in Table 3.

**FIGURE 2.** FTIR spectrum of oxy-schorl from Příbyslavice.**TABLE 3.** IR spectroscopic data for oxy-schorl from Příbyslavice

Peak (cm ⁻¹)	Assignment
400–840	lattice vibrations
840–1200	Si ₆ O ₁₈ stretching vibrations (Fe,Mg)-OH bending vibrations BO ₃ stretching vibrations
1200–2000	O-H stretching (at O3; overlapping peaks from variable configurations of Y- and Z-site cations around O3)
~3000–3600	O-H stretching (at O1; overlap of peaks from variable configurations of Y-site cations)
3600–3700	

Thermogravimetric analysis

Thermal decomposition of oxy-schorl from Zlatá Idka and Příbyslavice was studied in an inert atmosphere (Ar) using a simultaneous thermal analyzer (STA 449 C Jupiter, Netzsch) including both thermogravimetric analysis (TGA) and differential scanning calorimetry (DSC) in the range of 30–1100 °C at the Department of Inorganic Chemistry, Comenius University in Bratislava (Zlatá Idka) and Department of Physics, Palacký University in Olomouc (Příbyslavice). The sample from Zlatá Idka was placed into a Pt crucible with a lid and dynamically heated with a heating rate of 20 K/min. TG correction: 020/5000 mg, DSC correction: 020/50 mV. The Příbyslavice sample was dynamically heated in open alumina crucible with a heating rate of 5 K/min.

Powder X-ray diffraction

Powder XRD measurements of oxy-schorl from Zlatá Idka were made on the BRUKER D8 Advance diffractometer (Department of Mineralogy and Petrology, Faculty of Natural Sciences, Comenius University in Bratislava, Slovakia) under the following conditions: Bragg-Brentano geometry, Cu anticathode, NiKβ filters, accelerating voltage: 40 kV, beam current: 40 mA. Data were recorded by a BRUKER LynxEye detector. The step size was 0.01° 2θ, the step time was 5 s per one step, and the range of measurement was 4–65° 2θ. Measured data were fitted and lattice parameters were refined with the DIFFRAC^{plus} TOPAS software (Bruker 2012) using pseudo-Voigt function. Indexed diffraction data are listed in Table 4.

Powder XRD data for oxy-schorl from Příbyslavice were recorded with a PANalytical X'Pert PRO MPD diffractometer (CoKα radiation) in Bragg-Brentano geometry, equipped with an X'Celerator detector and programmable divergence and diffracted beam anti-scatter slits. A diffraction pattern of the sample on a zero-background Si slide was scanned with a step size of 0.017° in the 2θ range 5–90°. Data were indexed and refined with a Stoe WinXPow package (version 1.06), using built-in Treor (Werner et al. 1985) and least-square refinement routines (Stoe and Cie 1999). Indexed diffraction data are listed in Table 5.

Crystal-structure refinement

Single-crystal X-ray studies were carried out using a 4-circle Oxford Diffraction KM-4Xcalibur diffractometer with a Sapphire2 (large Be window) CCD detector. The CrySAlis (Oxford Diffraction) and SHELXTL (PC Version) (Sheldrick

¹ Brand, R.A. NORMOS: Mössbauer fitting program. URL: http://www.wissel-gmbh.de/index.php?option=com_docman&task=cat_view&gid=30&Itemid=164. Accessed: 2012-12-18. (Archived by WebCite at <http://www.webcitation.org/6D0MuoWYK>).

TABLE 4. Powder X-ray diffraction data for oxy-schorl from Zlatá Idka

<i>h k l</i>	<i>d</i> _{obs} (Å)	<i>I</i> (%)	<i>d</i> _{calc} (Å)	<i>h k l</i>	<i>d</i> _{obs} (Å)	<i>I</i> (%)	<i>d</i> _{calc} (Å)
1 0 1	6.314(1)	10	6.3130	1 0 4	1.7614(7)	6	1.7620
0 2 1	4.945(2)	8	4.9471	6 3 0	1.7356(8)	7	1.7364
0 3 0	4.592(2)	7	4.5940	0 7 2	1.7215(8)	4	1.7222
2 1 1	4.200(2)	25	4.2013	5 3 2	1.7215(8)	4	1.7222
2 2 0	3.977(2)	53	3.9785	0 2 4	1.7197(7)	5	1.7204
0 1 2	3.439(1)	53	3.4407	5 4 1	1.7119(8)	7	1.7126
1 3 1	3.365(1)	11	3.3664	2 6 2	1.6825(8)	9	1.6832
2 0 2	3.157(1)	3	3.1581	2 1 4	1.6809(7)	13	1.6815
4 0 1	3.099(1)	4	3.1003	0 8 1	1.6736(8)	6	1.6743
4 1 0	3.006(1)	13	3.0075	0 6 3	1.6484(7)	26	1.6490
1 2 2	2.934(1)	59	2.9354	6 0 3	1.6484(7)	26	1.6490
3 2 1	2.888(1)	6	2.8888	2 7 1	1.6377(8)	38	1.6384
3 1 2	2.602(1)	3	2.6025	2 5 3	1.6141(7)	3	1.6147
0 5 1	2.569(1)	100	2.5699	5 2 3	1.6141(7)	3	1.6147
0 0 3	2.3680(9)	14	2.3688	1 3 4	1.6105(7)	7	1.6111
2 3 2	2.361(1)	10	2.3621	5 5 0	1.5907(8)	48	1.5914
5 1 1	2.336(1)	13	2.3376	4 5 2	1.5798(7)	15	1.5805
5 0 2	2.177(1)	4	2.1779	4 0 4	1.5785(7)	6	1.5791
4 3 1	2.158(1)	8	2.1587	8 1 1	1.5724(7)	11	1.5731
3 0 3	2.1046(9)	4	2.1054	8 0 2	1.5495(7)	7	1.5502
0 3 3	2.1046(9)	4	2.1054	3 2 4	1.5483(6)	2	1.5489
4 2 2	2.0998(9)	2	2.1007	4 6 1	1.5425(7)	13	1.5432
2 2 3	2.0346(9)	37	2.0354	0 9 0	1.5307(7)	11	1.5313
1 5 2	2.0303(9)	41	2.0311	4 4 3	1.5228(7)	8	1.5234
1 6 1	2.0146(9)	10	2.0155	7 2 2	1.5209(7)	4	1.5216
4 4 0	1.9884(9)	3	1.9893	7 3 1	1.5143(7)	3	1.5150
3 4 2	1.9096(9)	54	1.9104	1 7 3	1.4454(6)	8	1.4459
4 1 3	1.8602(8)	3	1.8609	7 1 3	1.4454(6)	8	1.4459
1 4 3	1.8602(8)	3	1.8609	6 4 2	1.4438(7)	4	1.4444
6 2 1	1.8449(9)	9	1.8456	5 1 4	1.4428(6)	15	1.4433
3 3 3	1.7661(8)	8	1.7668				

Note: The five strongest lines are highlighted in bold.

TABLE 5. Powder X-ray diffraction data for oxy-schorl from Příbyslavice

<i>h k l</i>	<i>d</i> _{obs} (Å)	<i>I</i> (%)	<i>d</i> _{calc} (Å)	<i>h k l</i>	<i>d</i> _{obs} (Å)	<i>I</i> (%)	<i>d</i> _{calc} (Å)
1 0 1	6.364(4)	75	6.3604	0 2 4	1.7333(2)	2	1.7332
0 2 1	4.9775(7)	28	4.977	5 3 2	1.7312(1)	1.5	1.7312
3 0 0	4.616(1)	12	4.6149	2 6 2	1.6920(1)	1.9	1.692
2 1 1	4.2254(6)	48	4.225	6 0 3	1.6589(2)	14.1	1.659
2 2 0	3.9969(5)	52	3.9966	2 7 1	1.6461(1)	6.7	1.6461
0 1 2	3.4664(1)	100	3.4664	1 3 4	1.6227(3)	0.6	1.6225
1 3 1	3.3839(3)	6	3.384	5 5 0	1.5986(2)	7.3	1.5987
2 0 2	3.1803(2)	1	3.1802	4 0 4	1.5896(6)	2.4	1.5901
4 0 1	3.1164(3)	2	3.1163	8 1 1	1.5804(1)	0.7	1.5804
4 1 0	3.0211(3)	8	3.0212	3 2 4	1.5591(5)	1	1.5595
1 2 2	2.9549(1)	79	2.9549	4 6 1	1.5504(1)	1.9	1.5504
3 2 1	2.9035(2)	5	2.9034	9 0 0	1.5383(1)	1.8	1.5383
3 1 2	2.6188(3)	3	2.6186	7 2 2	1.5293(1)	1.6	1.5293
0 5 1	2.5826(1)	65	2.5826	7 3 1	1.5221(1)	0.8	1.5221
0 4 2	2.4883(3)	3	2.4885	8 2 0	1.5105(2)	2.6	1.5106
2 4 1	2.4576(2)	3	2.4575	0 5 4	1.5033(2)	9.3	1.5034
0 0 3	2.3868(2)	12	2.3869	2 4 4	1.4772(4)	2.3	1.4775
2 3 2	2.3761(2)	16	2.376	5 1 4	1.4528(2)	10.2	1.4529
5 1 1	2.3490(1)	9	2.349	7 4 0	1.4355(2)	1.6	1.4356
6 0 0	2.3072(4)	1	2.3075	0 1 5	1.4247(2)	3.1	1.4246
1 1 3	2.2869(3)	1	2.2871	6 5 1	1.4224(1)	3.5	1.4224
5 2 0	2.2171(3)	1	2.2169	4 3 4	1.4072(2)	6.6	1.4071
5 0 2	2.1903(2)	9	2.1904	3 8 1	1.3793(2)	0.6	1.3794
4 3 1	2.1692(2)	7	2.1691	10 0 1	1.3593(1)	3.8	1.3593
3 0 3	2.1200(2)	11	2.1201	9 1 2	1.3450(1)	2	1.345
4 2 2	2.1125(1)	4	2.1125	6 6 0	1.3321(2)	1.2	1.3322
2 2 3	2.0494(2)	12	2.0493	7 0 4	1.3277(5)	2.8	1.3273
1 5 2	2.0423(2)	31	2.0424	0 4 5	1.3234(0)	1.7	1.3234
1 6 1	2.0252(2)	5	2.0251	10 1 0	1.3140(2)	3.5	1.3141
4 4 0	1.9983(1)	2	1.9983	8 3 2	1.3087(2)	1	1.3085
3 4 2	1.9207(2)	17	1.9208	2 3 5	1.3055(2)	1.2	1.3056
7 0 1	1.9065(2)	2	1.9064	9 0 3	1.2931(2)	0.5	1.293
4 1 3	1.8729(1)	8	1.8729	0 10 2	1.2913(1)	0.7	1.2913
6 2 1	1.8545(2)	4	1.8544	8 4 1	1.2869(1)	0.8	1.2869
7 1 0	1.8340(3)	1	1.8338	9 3 0	1.2799(1)	1.3	1.2799
6 1 2	1.8186(2)	2	1.8187	8 2 3	1.2765(2)	1	1.2764
3 3 3	1.7779(1)	3	1.7779	5 0 5	1.2720(2)	4.1	1.2721
1 0 4	1.7754(1)	3	1.7754				

Note: The five strongest lines are highlighted in bold.

TABLE 6. Crystal and refinement data for oxy-schorl from Zlatá Idka

<i>a</i> = 15.916(3) Å	Space group: <i>R3m</i>
<i>c</i> = 7.1071(12) Å	MoK α radiation, λ = 0.71073 Å
<i>V</i> = 1559.1(4) Å ³	Cell parameters from 1225 reflections
<i>Z</i> = 3	
Elongated grain, brown	0.20 × 0.10 × 0.10 mm
θ = 3.2–36.1°	(−26 ≤ <i>h</i> ≤ 17, −17 ≤ <i>k</i> ≤ 26, −11 ≤ <i>l</i> ≤ 11)
μ = 1.68 mm ^{−1}	<i>F</i> (000) = 1468
<i>T</i> = 293 K	
Reflections measured:	3174
Independent reflections:	1474
Reflections >2 σ :	1111
<i>R</i> [<i>F</i> ² > 2 σ (<i>F</i> ²)] = 0.034	(Δ / σ) _{max} = <0.001
<i>wR</i> (<i>F</i> ²) = 0.066	extinction coef.: none
<i>S</i> = 0.84	92 parameters refined
$\Delta\rho_{max}$ = 0.67 e Å ^{−3}	$\Delta\rho_{min}$ = −0.38 e Å ^{−3}

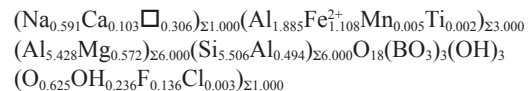
TABLE 7. Fractional atomic coordinates and isotropic or equivalent isotropic displacement parameters (Å²) of oxy-schorl from Zlatá Idka

	<i>x</i>	<i>y</i>	<i>z</i>	<i>U</i> _{iso} ² / <i>U</i> _{eq}	Occ. (<1)
Na	0.0000	0.0000	0.0825(5)	0.0229(12)	0.859(14)
Y (Al)	0.12237(7)	0.06118(4)	0.50346(13)	0.0119(3)	0.799(7)
Y (Fe)	0.12237(7)	0.06118(4)	0.50346(13)	0.0119(3)	0.201(7)
Z (Al)	0.29700(6)	0.36937(6)	1.14311(12)	0.0104(2)	0.959(5)
Si	0.19214(5)	0.19002(5)	0.86941(10)	0.0080(2)	0.899(5)
O1	0.0000	0.0000	0.6394(8)	0.0269(12)	
O2	0.06060(11)	0.1212(2)	0.3556(4)	0.0210(7)	
O3	0.2620(2)	0.13101(12)	0.3745(4)	0.0189(7)	
O4	0.1869(2)	0.09346(11)	0.9640(4)	0.0198(6)	
O5	−0.1883(2)	−0.09417(11)	−0.0580(4)	0.0192(6)	
O6	0.19549(14)	0.18438(14)	0.6403(3)	0.0150(4)	
O7	0.28759(14)	0.28731(13)	0.9447(3)	0.0142(4)	
O8	0.20909(14)	0.26975(14)	1.3046(3)	0.0145(4)	
B	0.10971(18)	0.2194(4)	0.3182(6)	0.0142(8)	

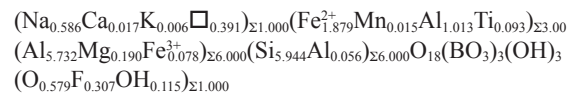
2000) program packages were used for data reduction and structure refinement, respectively, using neutral scattering factors and anomalous dispersion corrections. The structure of oxy-schorl was refined in *R3m* and converged to a final *R* index of 3.32% for Zlatá Idka and 1.91% for Příbyslavice data. Crystal and refinement details of tourmaline from Zlatá Idka are listed in Table 6, structural data are summarized in Tables 7 to 9, and the bond-valence table is presented in Table 10. Crystal and refinement details of tourmaline from Příbyslavice are listed in Table 11, and structural data are summarized in Tables 12 to 14; its bond-valence table is presented in Table 15. (CIF and data sets are deposited online².)

RESULTS

The samples of oxy-schorls from Zlatá Idka and Příbyslavice display some differences in chemical composition and site allocation. A combination of EMPA, Mössbauer spectroscopy and crystal-structure refinement yields following empirical formulas



and



² Deposit item AM-13-026, CIF and data sets. Deposit items are available two ways: For a paper copy contact the Business Office of the Mineralogical Society of America (see inside front cover of recent issue) for price information. For an electronic copy visit the MSA web site at <http://www.minsocam.org>, go to the *American Mineralogist* Contents, find the table of contents for the specific volume/issue wanted, and then click on the deposit link there.

TABLE 8. Atomic displacement parameters (\AA^2) of oxy-schorl from Zlatá Idka

	U^{11}	U^{22}	U^{33}	U^{12}	U^{13}	U^{23}
Na	0.0223(15)	0.0223(15)	0.024(2)	0.0111(8)	0.000	0.000
Y(Al)	0.0113(5)	0.0098(4)	0.0151(5)	0.0057(2)	-0.0019(3)	-0.00095(17)
Y(Fe)	0.0113(5)	0.0098(4)	0.0151(5)	0.0057(2)	-0.0019(3)	-0.00095(17)
Z(Al)	0.0113(4)	0.0109(4)	0.0098(4)	0.0060(3)	0.0001(3)	-0.0004(3)
Si	0.0081(4)	0.0082(4)	0.0076(3)	0.0041(3)	-0.0002(3)	-0.0008(3)
O1	0.0314(19)	0.0314(19)	0.018(3)	0.0157(9)	0.000	0.000
O2	0.0251(13)	0.0147(14)	0.0197(14)	0.0073(7)	0.0001(6)	0.0002(12)
O3	0.0291(17)	0.0171(11)	0.0144(13)	0.0146(8)	0.0005(12)	0.0003(6)
O4	0.0243(16)	0.0168(10)	0.0208(14)	0.0121(8)	-0.0001(12)	0.0000(6)
O5	0.0250(16)	0.0188(11)	0.0160(13)	0.0125(8)	0.0018(11)	0.0009(6)
O6	0.0165(10)	0.0169(10)	0.0111(8)	0.0080(8)	0.0012(7)	0.0008(7)
O7	0.0135(9)	0.0138(9)	0.0133(8)	0.0053(8)	0.0002(7)	-0.0003(7)
O8	0.0136(9)	0.0152(10)	0.0153(9)	0.0075(8)	-0.0001(7)	0.0018(7)
B	0.0172(16)	0.015(2)	0.0094(16)	0.0077(10)	-0.0002(7)	-0.0004(14)

TABLE 9. Selected bond lengths for oxy-schorl from Zlatá Idka

Site	Anion	Distance	s.d.	Site	Anion	Distance	s.d.	
X	O2*	2.561	(4)	Z	O6**	1.869	(2)	
	O2†	2.561	(4)		O7	1.876	(2)	
	O2	2.561	(4)		O8	1.889	(2)	
	O4‡	2.710	(3)		O8††	1.918	(2)	
	O4§	2.710	(3)		O7‡‡	1.925	(2)	
	O4	2.710	(3)		O3**	1.9890	(15)	
	O5*	2.781	(3)		avg.	1.911		
	O5†	2.781	(3)					
	O5	2.781	(3)		T	O7	1.625	(2)
	avg.	2.684				O5§§	1.6298	(12)
			O6	1.633		(2)		
Y	O1	1.944	(3)	B	O2	1.380	(6)	
	O6#	1.965	(2)		O8‡	1.373	(3)	
	O6	1.965	(2)		O8	1.373	(3)	
	O2	1.981	(2)		avg.	1.375		
	O2*	1.981	(2)					
	O3	2.132	(3)					
	avg.	1.995						

Symmetry codes:

* $-x+y, -x, z$ † $-y, x-y, z$ ‡ $x, y, z-1$ § $-y, x-y, z-1$ || $-x+y, -x, z-1$ # $x, x-y, z$ ** $-x+y+1/3, -x+2/3, z+2/3$ †† $-x+y+1/3, -x+2/3, z-1/3$ ‡‡ $-y+2/3, x-y+1/3, z+1/3$ §§ $-x+y, -x, z+1$ ||| $-x+y, y, z-1$

for oxy-schorl from Zlatá Idka and Příbyslavice, respectively. They are in good agreement with the end-member formula $\text{Na}(\text{Fe}_2^+\text{Al})\text{Al}_6\text{Si}_6\text{O}_{18}(\text{BO}_3)_3(\text{OH})_3\text{O}$ requiring SiO_2 35.22, Al_2O_3 34.87, FeO 14.04, Na_2O 3.03, B_2O_3 10.20, H_2O 2.64, total 100.00 wt%. As suggested by the empirical formulas, oxy-schorl from Zlatá Idka is moderately disordered in the octahedral sites, while disorder in oxy-schorl from Příbyslavice is only negligible.

The content of OH^- was calculated from an electroneutral formula based on the crystal-structure refinement and Mössbauer spectroscopy data. Ferric iron takes only 4% of all Fe in oxy-schorl from Příbyslavice and it was not detected in the sample from Zlatá Idka. The content of H_2O was also measured using TGA; the TGA curve shows a mass change -2.96% (Zlatá Idka) and -2.69% (Příbyslavice) at ca. 950–1020 °C, which corresponds to breakdown of the structure and release of water (bound in form of OH^-). Reduced content of $^{\text{H}}\text{OH}$ is also supported by the low intensity of the O–H stretching peak at 3628

TABLE 10. Bond valence table for oxy-schorl from Zlatá Idka

	X	Y	Z	B	T	Σ
	$\text{Na}_{0.591}\text{Ca}_{0.103}$ $\text{K}_{0.004}\square_{0.302}$	$\text{Al}_{1.808}\text{Fe}_{1.105}$ $\text{Ti}_{0.002}\text{Mn}_{0.005}\text{Mg}_{0.079}$	$\text{Al}_{5.5}\text{Mg}_{0.5}$	B	$\text{Si}_{5.509}\text{Al}_{0.491}$	
O1*		0.478				1.435
O2	0.098	0.450		0.946		1.973
	0.098	0.450				
	0.098					
O3*		0.299	0.405			1.109
O4	0.065				0.960	1.986
	0.065					
	0.065					
O5	0.054				0.991	2.035
	0.054					
	0.054					
O6	0.469		0.560		0.982	2.012
	0.469					
O7			0.550		1.003	2.035
			0.482			
O8			0.531	0.995		2.016
			0.491	0.995		
Σ	0.649	2.616	3.019	2.965	3.937	
IC(avg.)	0.801	2.603	2.917	3.000	3.918	
Δ	0.152	-0.013	-0.102	0.035	-0.019	

Note: IC(avg.) = average ionic charge of atoms occupying the site.

* Hydrogen bond donor.

† Content of the O1 site is: $\text{O}_{0.536}\text{OH}_{0.328}\text{F}_{0.136}$.**TABLE 11.** Crystal and refinement data for oxy-schorl from Příbyslavice

$a = 15.9853(12)$ Å	Space group: $R\bar{3}m$
$c = 7.1538(6)$ Å	MoK α radiation, $\lambda = 0.71073$ Å
$V = 1583.1(2)$ Å ³	Cell parameters from 2936 reflections
$Z = 3$	
Elongated grain, brown	$0.30 \times 0.10 \times 0.10$ mm
$\theta = 2.9\text{--}36.1^\circ$	$-26 \leq h \leq 18, -25 \leq k \leq 23, -8 \leq l \leq 11$
$\mu = 2.20$ mm ⁻¹	$F(000) = 1501$
$T = 293$ K	
Reflections measured	4166
Independent reflections	1380
Reflections $> 2\sigma$	1285
$R [F^2 > 2\sigma(F^2)] = 0.0191$	$(\Delta/\sigma)_{\text{max}} = 0.001$
$wR(F^2) = 0.0400$	extinction coef. = 0.00058(10)
$S = 0.98$	96 parameters refined
$\Delta\rho_{\text{max}} = 0.65$ e Å ⁻³	$\Delta\rho_{\text{min}} = -0.49$ e Å ⁻³

TABLE 12. Fractional atomic coordinates and isotropic or equivalent isotropic displacement parameters (\AA^2) for oxy-schorl from Příbyslavice

Site	x/a	y/b	z/c	$U_{\text{iso}}^*/U_{\text{eq}}$	Occ.	
X Na	0	0	0.9019(5)	0.0266(11)	0.676(10)	
Y Fe	0.87496(3)	0.937481(16)	0.50264(6)	0.00869(12)	0.621(4)	
	Al	0.87496(3)	0.937481(16)	0.50264(6)	0.00869(12)	0.379(4)
Z Al	0.70355(3)	0.63191(3)	-0.14783(6)	0.00590(13)	0.974(3)	
	Fe	0.70355(3)	0.63191(3)	-0.14783(6)	0.00590(13)	0.026(3)
T Si	0.80806(3)	0.81008(3)	0.12963(6)	0.00569(10)		
O1	O1	0	0	0.3485(5)	0.0363(9)	0.69†
	F	0	0	0.3485(5)	0.0363(9)	0.31†
O2	O2	0.93822(6)	0.87643(12)	0.6435(3)	0.0151(4)	
O3	O3	0.73144(14)	0.86572(7)	0.6201(2)	0.0123(3)	
O4	O4	0.81267(12)	0.90634(6)	0.0387(2)	0.0103(3)	
O5	O5	0.18631(12)	0.09316(6)	0.0618(2)	0.0104(3)	
O6	O6	0.80182(8)	0.81238(8)	0.35415(17)	0.0089(2)	
O7	O7	0.71481(8)	0.71419(8)	0.05039(16)	0.0086(2)	
O8	O8	0.79017(8)	0.72936(8)	-0.31139(16)	0.0097(2)	
B B	0.88991(10)	0.77981(19)	0.6753(4)	0.0076(4)		
H3 H3	0.735(2)	0.8677(12)	0.732(5)	0.21(2)*		

* Isotropic displacement parameter (\AA^2).

† Fixed according to EMPA analyses.

cm⁻¹ in the infrared absorption spectrum (Fig. 2). With regard to the possible chemical inhomogeneity of the samples (Fig. 1), the calculated H_2O contents were preferred to the TGA results.

TABLE 13. Anisotropic displacement parameters (\AA^2) for oxy-schorl from Příbyslavice

Site	U_{11}	U_{22}	U_{33}	U_{12}	U_{13}	U_{23}
X	0.0267(13)	0.0267(13)	0.0263(18)	0.0134(7)	0	0
Y	0.0087(2)	0.00611(15)	0.0121(2)	0.00433(10)	-0.00216(15)	-0.00108(7)
Z	0.0062(2)	0.0058(2)	0.0058(2)	0.00309(18)	0.00034(15)	-0.00008(16)
T	0.0054(2)	0.00520(19)	0.0064(2)	0.00266(15)	-0.00021(15)	-0.00044(14)
O1	0.0494(15)	0.0494(15)	0.0102(15)	0.0247(8)	0	0
O2	0.0207(7)	0.0069(7)	0.0132(8)	0.0035(4)	0.0004(3)	0.0008(6)
O3	0.0213(9)	0.0123(6)	0.0063(7)	0.0107(4)	0.0007(6)	0.0004(3)
O4	0.0145(8)	0.0074(5)	0.0114(8)	0.0072(4)	0.0011(6)	0.0006(3)
O5	0.0149(8)	0.0082(5)	0.0105(7)	0.0075(4)	0.0012(6)	0.0006(3)
O6	0.0090(5)	0.0103(5)	0.0070(5)	0.0047(4)	-0.0003(4)	-0.0009(4)
O7	0.0088(5)	0.0068(5)	0.0082(5)	0.0024(4)	-0.0009(4)	-0.0008(4)
O8	0.0075(5)	0.0115(5)	0.0111(5)	0.0054(5)	0.0010(4)	0.0021(4)
B	0.0077(7)	0.0074(10)	0.0074(10)	0.0037(5)	0.0000(4)	0.0000(8)

TABLE 14. Selected bond lengths for oxy-schorl from Příbyslavice

Site	Anion	Distance	s.d.	Site	Anion	Distance	s.d.	
X	O2*	2.519	(3)	Z	O6***	1.8615	(13)	
	O2†	2.519	(3)		O7	1.8804	(12)	
	O2‡	2.519	(3)		O8	1.8857	(12)	
	O4§	2.772	(2)		O8†††	1.9264	(12)	
	O4	2.772	(2)		O7‡‡‡	1.9589	(12)	
	O4#	2.772	(2)		O3***	1.9814	(9)	
	O5**	2.821	(2)		avg.	1.916		
	O5††	2.821	(2)					
	O5‡‡	2.821	(2)		T	O6	1.6108	(13)
	O5‡‡	2.821	(2)			O7	1.6149	(11)
avg.	2.704		O5§§§§	1.6253		(7)		
			O4	1.638		(8)		
Y	O2	1.9941	(12)	B	O2	1.357	(3)	
	O2§§	1.9942	(12)		O8††	1.3841	(18)	
	O6	2.0387	(13)		O8	1.3841	(18)	
	O6	2.0387	(13)		avg.	1.375		
	O1##	2.052	(2)					
	O3	2.1572	(19)					
avg.	2.046							

Symmetry codes:

- * $x-1, y-1, z$
- † $-x+y, -x+1, z$
- ‡ $-y+1, x-y, z$
- § $-x+y, -x+1, z+1$
- || $x-1, y-1, z+1$
- # $-y+1, x-y, z+1$
- ** $-y, x-y, z+1$
- †† $x, y, z+1$
- ‡‡ $-x+y, -x, z+1$
- §§ $-x+y+1, -x+2, z$
- |||| $x, x-y+1, z$
- ## $x+1, y+1, z$
- *** $-x+y+2/3, -x+4/3, z-2/3$
- ††† $-x+y+2/3, -x+4/3, z+1/3$
- ‡‡‡ $-y+4/3, x-y+2/3, z-1/3$
- §§§ $-x+y+1, -x+1, z$
- ||||| $-x+y+1, y, z+1$.

Both tourmalines slightly differ structurally as represented by lattice parameters: $a = 15.9074(9) \text{ \AA}$, $c = 7.1039(2) \text{ \AA}$, $V = 1557.4(2) \text{ \AA}^3$ (powder XRD) and $a = 15.916(3) \text{ \AA}$, $c = 7.107(1) \text{ \AA}$, $V = 1559.1(4) \text{ \AA}^3$ (crystal-structure refinement) for Zlatá Idka and $a = 15.9865(8) \text{ \AA}$, $c = 7.1608(3) \text{ \AA}$, $V = 1584.9(2) \text{ \AA}^3$ (powder XRD) and $a = 15.985(1) \text{ \AA}$, $c = 7.154(1) \text{ \AA}$, $V = 1583.1(2) \text{ \AA}^3$ (crystal-structure refinement) for Příbyslavice. Differences in lattice parameters result from different Fe^{2+} , Fe^{3+} , and Al^{3+} occupancies in Y, Z, and T sites in both tourmalines.

Despite all differences between studied samples, they both belong to alkali group (Fig. 3a), they represent oxy species (Fig. 3b) and their contents of Fe and Mg correspond to the composition of oxy-schorl (Fig. 3c).

TABLE 15. Bond-valence table for oxy-schorl from Příbyslavice

	X	Y	Z	B	T	Σ
O1*		0.363				1.088
O2	0.091	0.466		1.039		2.063
	0.091	0.466				
	0.091					
O3*		0.298	0.411			1.119
O4	0.046				0.965	1.975
	0.046					
	0.046					
O5	0.040				0.997	2.033
	0.040					
O6		0.415	0.571		1.033	2.020
		0.415				
O7			0.545		1.021	2.005
			0.439			
O8			0.535	0.964		1.978
			0.480	0.964		
			2.980	2.966	4.015	
Σ	0.531	2.423	2.980	2.966	4.015	
IC(avg.)	0.632	2.400	2.968	3.000	3.991	
Δ	0.101	-0.024	-0.012	0.034	-0.025	

Note: IC(avg.) = average ionic charge of atoms occupying the site.

* Hydrogen bond donor.

DISCUSSION AND CONCLUSIONS

Oxy-schorl is chemically and structurally related to schorl. The name oxy-schorl has been abundantly used for tourmalines with the composition similar to schorl but containing more than 6.5 apfu Al, and O in the W site if known (e.g., Hawthorne and Henry 1999; Henry and Dutrow 2001; Buriánek and Novák 2004, 2007; Novák et al. 2004; Ertl et al. 2010a, 2010b; Bakshiev et al. 2011; Bosi 2011). Since the current classification of the tourmaline supergroup (Henry et al. 2011) uses ordered formulas for tourmaline classification, it is generally possible to recognize oxy-schorl from electron microprobe data using the approximate limits: $\text{Na} > 0.5$ apfu, $\text{Al} > 6.5$ apfu, $\text{Fe} > \text{Mg}$, and $\text{F} < 0.5$ apfu. However, ordering of ions in the structure of different samples can be variable. In the tourmaline structure, the W site is located on the threefold axis passing through the unit cell, and surrounded by three Y sites (Hawthorne 1996, 2002). From the crystallographic point of view there are two different possible arrangements: (1) $W = \text{OH}$ or F with valence bond ca. 0.33 v.u.; (2) $W = \text{O}$ -valence bond is ca. 0.67 v.u. (v.u. = valence units, Hawthorne 1996, 2002). The substitution of O for OH results in the increase of charge requirements in the neighboring Y sites and the substitution of Al for divalent cations, or disorder of divalent and trivalent cations among the octahedral Y and Z sites. If the W site is fully occupied by O, the structural arrangements with 3^YR^{2+} or $2^Y\text{R}^{2+}+^Y\text{R}^{3+}$ cations are less favorable than the arrangements with 3^YR^{3+} or $2^Y\text{R}^{3+}+^Y\text{R}^{2+}$ (Hawthorne 2002). Therefore, in natural samples with the mixed occupancy of the W site, combination of $2^Y\text{R}^{2+}+^Y\text{R}^{3+}$ and $2^Y\text{R}^{3+}+^Y\text{R}^{2+}$ arrangements is the most probable.

The crystal-structure refinement of oxy-schorl from Zlatá Idka showed that a significant amount of divalent cations is located in the Z site, resulting in the content of $^Y\text{Al}^{3+}$ of 1.885 apfu, the possible Y site short-range arrangements favor dominant O^{2-} in the W site. The observed Al-Mg disorder in tourmalines was already studied (e.g., Grice and Ercit 1993; Hawthorne et al. 1993; Bloodaxe et al. 1999; Bosi and Lucchesi 2004). Although the Fe^{2+} - Al^{3+} disorder could be allowed by local short- and long-

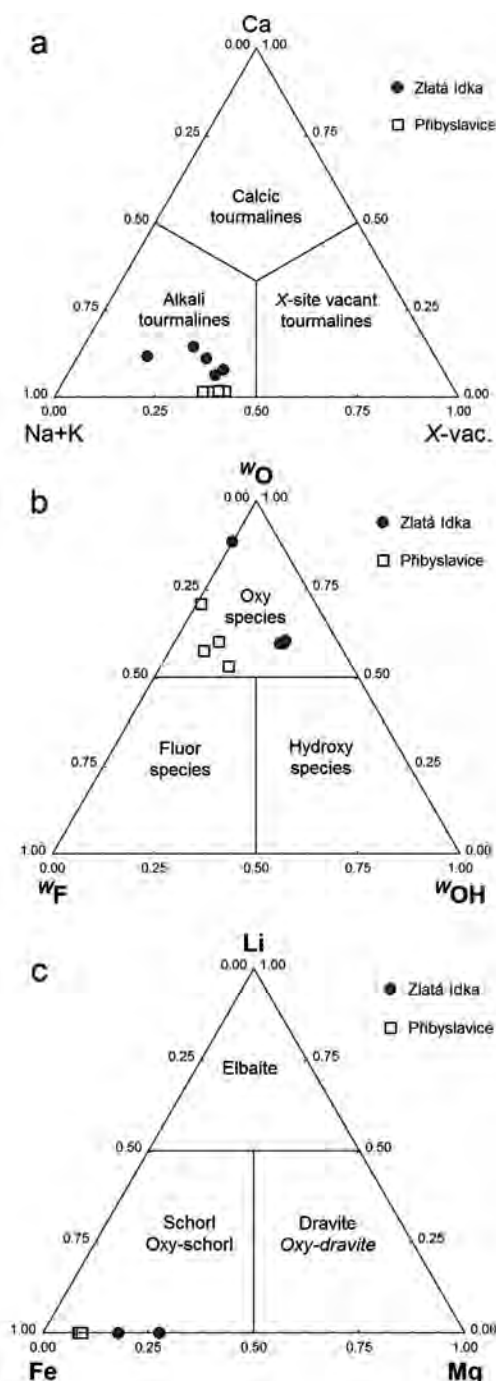


FIGURE 3. Ternary diagrams for minerals of tourmaline group used for determination of dominant occupancy at the *X* (a), *W* (b), and *Y* site (c).

range arrangements (Bosi 2011), Mg is more likely substituting for Al in the *Z* site due to its smaller ionic radii similar to Al^{3+} , as was observed in the oxy-schorl from Zlatá Idka. In contrast, the oxy-schorl from Příbyslavice shows only negligible disorder of Al and (Mg,Fe) in octahedral sites; the vast majority of R^{2+} ($\text{Fe}^{2+} \gg \text{Mg}$) is allocated to the *Y* site. However, the calculated bond valence values for the O1 and O3 sites suggest a disorder of O

and OH among the anion sites *V* and *W* (Table 15).

The formula of end-member oxy-schorl may be expressed either as $\text{Na}(\text{Fe}^{2+}\text{Al}_2)(\text{Fe}^{2+}\text{Al}_3)\text{Si}_6\text{O}_{18}(\text{BO}_3)_3(\text{OH})_3\text{O}$ with cations disordered in two structural sites, or with cations disordered only in one structural site such as $\text{NaAl}_3(\text{Al}_4\text{Fe}_2^{2+})\text{Si}_6\text{O}_{18}(\text{BO}_3)_3(\text{OH})_3\text{O}$ and $\text{Na}(\text{Fe}_2^{2+}\text{Al})\text{Al}_6\text{Si}_6\text{O}_{18}(\text{BO}_3)_3(\text{OH})_3\text{O}$, the formula used in the valid nomenclature (Henry et al. 2011). It recommends the allocation of trivalent cations to the *Z* site initially, followed by the assignment of the remainder of R^{3+} to the *Y* site. Nevertheless, this end-member formula could not be stable owing to the local charge requirements, and the first formula with cations disordered in two sites is closely approaching the composition of natural samples (Hawthorne 2002).

These two studied oxy-schorl samples confirm the two distinct ordering mechanisms in natural oxy-tourmalines: (1) disorder of divalent and trivalent cations in octahedral sites and all O ordered in the *W* site (favored by the Mg-bearing oxy-schorl from Zlatá Idka); (2) cations ordered in the *Y* and *Z* sites and O disordered in the *V* and *W* sites (in Fe-dominant oxy-schorl from Příbyslavice). The elevated content of Mg in the oxy-schorl from Zlatá Idka (Fig. 3c, Table 1) very likely facilitates a higher degree of disorder in *Y* and *Z* sites and a higher ordering in the *W* site relative to a Mg-poor oxy-schorl from Příbyslavice. Since a formula with ordered *V* and *W* sites is recommended for classification purposes (Henry et al. 2011), both compositions result in the same ordered formula that meets nomenclatural requirements for oxy-schorl.

The presence of oxy-schorl does not necessarily imply an oxidizing geological environment. The mineral association in the Příbyslavice orthogneiss suggests more reductive conditions documented by magnetite and pyrite (e.g., Povondra et al. 1987, 1998). Thus the reasons of the formation of oxy-schorl in spite of the presence of schorl are different than the high oxygen fugacity. The latter could take a role in oxy-tourmalines with an increased proportion of Fe^{3+} as buergerite (e.g., Donnay et al. 1966; Grice and Ercit 1993) or povondraite component (e.g., Grice et al. 1993; Bačík et al. 2008; Baksheev et al. 2011; Novák et al. 2011), respectively, in which the deprotonization is driven by a ${}^Y\text{Fe}^{2+}+{}^{W+V}\text{OH}^- \leftrightarrow {}^Y\text{Fe}^{3+}+{}^{W+V}\text{O}^{2-}$ reaction (Piecza and Kraczk 2004; Bačík et al. 2011). In contrast, the deprotonization was driven by ${}^Y\text{R}^{2+}+{}^{W+V}\text{OH}^- \leftrightarrow {}^Y\text{Al}+{}^{W+V}\text{O}^{2-}$ reaction in the studied samples of oxy-schorl from both localities. Consequently, the deprotonization in studied oxy-schorls was likely the result of local charge-balance requirements owing to the excess of Al and the formation of Al-enriched oxy-schorl is the result of the specific geochemistry of the host rock.

ACKNOWLEDGMENTS

Authors thank Tomáš Vaculovič for LA-ICP-MS analysis. This work was supported by projects APVV-VVCE-0033-07 to P.B., P.U., and D.O. and GAP210/10/0743 to J.C., J.F., M.N., and R.S. and by the Operational Program Research and Development for Innovations—European Regional Development Fund (Project No. CZ.1.05/2.1.00/03.0058 of the Ministry of Education, Youth and Sports of the Czech Republic) to J.F. We thank Martin Kunz and Fernando Colombo for editorial handling and for detailed reviews and fruitful discussion.

REFERENCES CITED

- Bačík, P., Uher, P., Sýkora, M., and Lipka, J. (2008) Low-Al tourmalines of the schorl-dravite-povondraite series in redeposited tourmalinites from the Western Carpathians, Slovakia. *Canadian Mineralogist*, 46, 1117–1129.
- Bačík, P., Ozdín, D., Miglierini, M., Kardošová, P., Penrák, M., and Haloda, J.

- (2011) Crystallochemical effects of heat treatment on Fe-dominant tourmalines from Dolní Bory (Czech Republic) and Vlachovo (Slovakia). *Physics and Chemistry of Minerals*, 38, 599–611.
- Bakshiev, I.A., Prokof'ev, V.Y., Yapaskurt, V.O., Viganas, M.F., Zorina, L.D., and Solov'ev, V.N. (2011) Ferric-iron-rich tourmaline from the Darasun gold deposit, Transbaikalia, Russia. *Canadian Mineralogist*, 49, 263–276.
- Bloodaxe, E.S., Hughes, J.M., Dyar, M.D., Grew, E.S., and Guidotti, C.V. (1999) Linking structure and chemistry in the schorl-dravite series. *American Mineralogist*, 84, 922–928.
- Bosi, F. (2011) Stereochemical constraints in tourmaline: From a short-range to a long-range structure. *Canadian Mineralogist*, 49, 17–27.
- Bosi, F. and Lucchesi, S. (2004) Crystal chemistry of the schorl-dravite series. *European Journal of Mineralogy*, 16, 335–344.
- Breiter, K., Škoda, R., and Novák, M. (2010) Field stop 5: Příbyslavice near Čáslav – complex of peraluminous phosphorus-rich tourmaline-bearing orthogneiss, and associated granite and pegmatite with garnet, tourmaline, and primary Fe-Mn phosphates. In M. Novák and J. Cempírek, Eds., *Granitic Pegmatites and Mineralogical Museums in the Czech Republic*, vol. 6, p. 29–36. *Acta Mineralogica-Petrographica, Field Guide Series*, Szeged, Hungary.
- Bruker (2012) DIFFRAC.SUITE TOPAS, XRD Software. <http://www.bruker.com/products/x-ray-diffraction-and-elemental-analysis/x-ray-diffraction/xrd-software/applications/xrd-software-applications/topas.html>. Accessed: 2012-12-18. (Archived by WebCite at <http://www.webcitation.org/6D0LfZQDt>).
- Buriánek, D. and Novák, M. (2004) Morphological and compositional evolution of tourmaline from nodular granite at Lavičky near Velké Meziříčí, Moldanubicum, Czech Republic. *Journal of Czech Geological Society*, 49, 81–90.
- (2007) Compositional evolution and substitutions in disseminated and nodular tourmaline from leucocratic granites: Examples from the Bohemian Massif, Czech Republic. *Lithos*, 95, 148–164.
- Donnay, G., Ingamells, C.O., and Mason, B. (1966) Buergerite, a new species of tourmaline. *American Mineralogist*, 51, 198–199.
- Ertl, A., Marschall, H.R., Giester, G., Henry, D.J., Schertl, H.P., Ntaflou, T., Luvi-zotto, G.L., Nasdala, L., and Tillmanns, E. (2010a) Metamorphic ultrahigh-pressure tourmaline: Structure, chemistry, and correlations to *P-T* conditions. *American Mineralogist*, 95, 1–10.
- Ertl, A., Rossman, G.R., Hughes, J.M., London, D., Wang, Y., O'Leary, J.A., Dyar, M.D., Prowatke, S., Ludwig, T., and Tillmanns, E. (2010b) Tourmaline of the elbaite-schorl series from the Himalaya Mine, Mesa Grande, California: A detailed investigation. *American Mineralogist*, 95, 24–40.
- Foit, F.F. Jr. (1989) Crystal chemistry of alkali-deficient schorl and tourmaline structural relationships. *American Mineralogist*, 74, 422–431.
- Foit, F.F. Jr. and Rosenberg, P.E. (1977) Coupled substitutions in the tourmaline group. *Contributions to Mineralogy and Petrology*, 62, 109–127.
- Grice, J.D. and Ercit, T.S. (1993) Ordering of Fe and Mg in tourmaline: The correct formula. *Neues Jahrbuch für Mineralogie Abhandlungen*, 165, 245–266.
- Grice, J.D., Ercit, T.S., and Hawthorne, F.C. (1993) Povondraite, a redefinition of the tourmaline ferridravite. *American Mineralogist*, 78, 433–436.
- Hawthorne, F.C. (1996) Structural mechanisms for light elements in tourmaline. *Canadian Mineralogist*, 34, 123–132.
- (2002) Bond-valence constraints on the chemical composition of tourmaline. *Canadian Mineralogist*, 40, 789–797.
- Hawthorne, F.C. and Henry, D.J. (1999) Classification of the minerals of the tourmaline group. *European Journal of Mineralogy*, 11, 201–215.
- Hawthorne, F.C., MacDonald, D.J., and Burns, P.C. (1993) Reassignment of cation site occupancies in tourmaline: Al-Mg disorder in the crystal structure of dravite. *American Mineralogist*, 78, 265–270.
- Henry, D.J. and Dutrow, B. (2001) Compositional zoning and element partitioning of nickeloan tourmaline in a metamorphosed karstbauxite from Samos, Greece. *American Mineralogist*, 86, 1130–1142.
- Henry, D., Novák, M., Hawthorne, F.C., Ertl, A., Dutrow, B., Uher, P., and Pezzotta, F. (2011) Nomenclature of the tourmaline supergroup-minerals. *American Mineralogist*, 96, 895–913.
- Novák, M., Povondra, P., and Selway, J.B. (2004) Schorl-oxy-schorl to dravite-oxy-dravite tourmaline from granitic pegmatites; examples from the Moldanubicum, Czech Republic. *European Journal of Mineralogy*, 16, 323–333.
- Novák, M., Škoda, R., Filip, J., Macek, I., and Vaculovič, T. (2011) Compositional trends in tourmaline from intragranitic NYF pegmatites of the Třebíč Pluton, Czech Republic: electron microprobe, Mössbauer and LA-ICP-MS study. *Canadian Mineralogist*, 49, 359–380.
- Pieczka, A. and Kraczká, J. (2004) Oxidized tourmalines—a combined chemical, XRD and Mössbauer study. *European Journal of Mineralogy*, 16, 309–321.
- Povondra, P. (1981) The crystal chemistry of tourmalines of the schorl-dravite series. *Acta Universitatis Carolinae, Geologica*, 223–264.
- Povondra, P., Čech, F., and Staněk, J. (1985) Crystal chemistry of elbaites from some pegmatites of the Czech Massif. *Acta Universitatis Carolinae, Geologica*, 1–24.
- Povondra, P., Pivec, E., Čech, F., Lang, M., Novák, F., Prachař, I., and Ulrych, J. (1987) Příbyslavice peraluminous granite. *Acta Universitatis Carolinae, Geologica*, 183–283.
- Povondra, P., Lang, M., Pivec, E., and Ulrych, J. (1998) Tourmaline from the Příbyslavice peraluminous alkali-feldspar granite, Czech Republic. *Journal of Czech Geological Society*, 43, 3–8.
- Reddy, B.J., Frost, R.L., Martens, W.N., Wain, D.L., and Klopogge, J.T. (2007) Spectroscopic characterization of Mn-rich tourmalines. *Vibrational Spectroscopy*, 44, 42–49.
- Sheldrick, G.M. (2000) SHELXTL, ver. 6.10. Bruker AXS Inc., Madison, Wisconsin.
- Stoe and Cie (1999) WinXPow. Stoe & Cie, Darmstadt, Germany.
- Vozárová, A., Šarinová, K., Larionov, A., Presnyakov, S., and Sergeev, S. (2010) Late Cambrian/Ordovician magmatic arc type volcanism in the Southern Gemericum basement, Western Carpathians, Slovakia: U-Pb (SHRIMP) data from zircons. *International Journal of Earth Sciences*, 99 (Suppl. 1), 17–37.
- Werner, P.-E., Eriksson, L., and Westdahl, M. (1985) TREOR, a semi-exhaustive trial-and-error powder indexing program for all symmetries. *Journal of Applied Crystallography*, 18, 367–370.
- Žák, T. and Jirásková, Y. (2006) CONFIT: Mössbauer spectra fitting program. *Surface and Interface Analysis*, 38, 710–714.

MANUSCRIPT RECEIVED JUNE 29, 2012

MANUSCRIPT ACCEPTED OCTOBER 11, 2012

MANUSCRIPT HANDLED BY FERNANDO COLOMBO


```

data_cemp_z1
_audit_update_record
;
2011-11-29 # Formatted by publCIF
;

_audit_creation_method          SHELXL-97
_chemical_name_systematic
?
_chemical_name_mineral      'oxy-schorl'
_chemical_compound_source  'Zlat. Idka, Slovakia'
_chemical_formula_sum
;
Al7.81 B3 Ca0.10 Cl0 F0.14 Fe1.11 H3.24 Mg0.57 Mn0.01 Na0.59 O30.86 Si5.51
;
_chemical_formula_weight      991.23

loop_
_atom_type_symbol
_atom_type_description
_atom_type_scatter_dispersion_real
_atom_type_scatter_dispersion_imag
_atom_type_scatter_source
'O'  'O'  0.0106  0.0060
'International Tables Vol C Tables 4.2.6.8 and 6.1.1.4'
'Na'  'Na'  0.0362  0.0249
'International Tables Vol C Tables 4.2.6.8 and 6.1.1.4'
'Fe'  'Fe'  0.3463  0.8444
'International Tables Vol C Tables 4.2.6.8 and 6.1.1.4'
'Al'  'Al'  0.0645  0.0514
'International Tables Vol C Tables 4.2.6.8 and 6.1.1.4'
'Si'  'Si'  0.0817  0.0704
'International Tables Vol C Tables 4.2.6.8 and 6.1.1.4'
'B'   'B'   0.0013  0.0007
'International Tables Vol C Tables 4.2.6.8 and 6.1.1.4'
'Mg'  'Mg'  0.0486  0.0363
'International Tables Vol C Tables 4.2.6.8 and 6.1.1.4'
'Ti'  'Ti'  0.2776  0.4457
'International Tables Vol C Tables 4.2.6.8 and 6.1.1.4'
'Mn'  'Mn'  0.3368  0.7283
'International Tables Vol C Tables 4.2.6.8 and 6.1.1.4'
'Ca'  'Ca'  0.2262  0.3064
'International Tables Vol C Tables 4.2.6.8 and 6.1.1.4'
'Cl'  'Cl'  0.1484  0.1585
'International Tables Vol C Tables 4.2.6.8 and 6.1.1.4'
'F'   'F'   0.0171  0.0103
'International Tables Vol C Tables 4.2.6.8 and 6.1.1.4'
'H'   'H'   0.0000  0.0000
'International Tables Vol C Tables 4.2.6.8 and 6.1.1.4'

_symmetry_cell_setting          trigonal
_symmetry_space_group_name_H-M  'R 3 m'

loop_
_symmetry_equiv_pos_as_xyz

```

```

'x, y, z'
'-y, x-y, z'
'-x+y, -x, z'
'-y, -x, z'
'-x+y, y, z'
'x, x-y, z'
'x+2/3, y+1/3, z+1/3'
'-y+2/3, x-y+1/3, z+1/3'
'-x+y+2/3, -x+1/3, z+1/3'
'-y+2/3, -x+1/3, z+1/3'
'-x+y+2/3, y+1/3, z+1/3'
'x+2/3, x-y+1/3, z+1/3'
'x+1/3, y+2/3, z+2/3'
'-y+1/3, x-y+2/3, z+2/3'
'-x+y+1/3, -x+2/3, z+2/3'
'-y+1/3, -x+2/3, z+2/3'
'-x+y+1/3, y+2/3, z+2/3'
'x+1/3, x-y+2/3, z+2/3'

```

```

_cell_length_a          15.916(3)
_cell_length_b          15.916(3)
_cell_length_c          7.1071(12)
_cell_angle_alpha       90.00
_cell_angle_beta        90.00
_cell_angle_gamma       120.00
_cell_volume            1559.1(4)
_cell_formula_units_Z   3
_cell_measurement_temperature 293(2)
_cell_measurement_reflns_used 1225
_cell_measurement_theta_min 3.2
_cell_measurement_theta_max 36.1

```

```

_exptl_crystal_description 'elongated grain'
_exptl_crystal_colour      'brown'
_exptl_crystal_size_max    0.2
_exptl_crystal_size_mid    0.1
_exptl_crystal_size_min    0.1
_exptl_crystal_density_meas ?
_exptl_crystal_density_diffn 3.167
_exptl_crystal_density_method 'not measured'
_exptl_crystal_F_000      1468
_exptl_absorpt_coefficient_mu 1.675
_exptl_absorpt_correction_T_min 0.87503
_exptl_absorpt_correction_T_max 1.00000
_exptl_absorpt_correction_type multi-scan
_exptl_absorpt_process_details
;

```

```

Crysalis RED, Oxford Diffraction Ltd.,
Version 1.171.33.52 (release 06-11-2009 Crysalis171 .NET)
(compiled Nov 6 2009,16:24:50)
Empirical absorption correction using spherical harmonics,
implemented in SCALE3 ABSPACK scaling algorithm.
;

```

```

_diffn_ambient_temperature 293(2)

```

```

_diffrn_radiation_wavelength      0.71073
_diffrn_radiation_type            'Mo K\alpha'
_diffrn_radiation_source          'Enhance (Mo) X-ray Source'
_diffrn_radiation_monochromator    'graphite'
_diffrn_measurement_device_type    'Kuma KM-4/Xcalibur-CCD(Sapphire2)'
_diffrn_measurement_method        '\w scans'
_diffrn_detector_area_resol_mean   8.4353
_diffrn_reflns_number             3174
_diffrn_reflns_av_R_equivalents   0.0381
_diffrn_reflns_av_sigmaI/netI    0.0780
_diffrn_reflns_limit_h_min        -26
_diffrn_reflns_limit_h_max        17
_diffrn_reflns_limit_k_min        -17
_diffrn_reflns_limit_k_max        26
_diffrn_reflns_limit_l_min        -11
_diffrn_reflns_limit_l_max        11
_diffrn_reflns_theta_min          3.22
_diffrn_reflns_theta_max          36.05
_reflns_number_total              1474
_reflns_number_gt                 1111
_reflns_threshold_expression      >2sigma(I)

_computing_data_collection
;
CrysAlis CCD, Oxford Diffraction Ltd.,
Version 1.171.33.52
;
_computing_cell_refinement
;
CrysAlis RED, Oxford Diffraction Ltd.,
Version 1.171.33.52
;
_computing_data_reduction
;
CrysAlis RED, Oxford Diffraction Ltd.,
Version 1.171.33.52
;
_computing_structure_solution      'SHELXS-97 (Sheldrick, 2008)'
_computing_structure_refinement    'SHELXL-97 (Sheldrick, 2008)'
_computing_publication_material    'SHELXL-97 (Sheldrick, 2008)'

_refine_special_details
;
Refinement of F2 against ALL reflections. The weighted R-factor wR and
goodness of fit S are based on F2, conventional R-factors R are based
on F, with F set to zero for negative F2. The threshold expression of
F2 > 2sigma(F2) is used only for calculating R-factors(gt) etc. and is
not relevant to the choice of reflections for refinement. R-factors based
on F2 are statistically about twice as large as those based on F, and R-
factors based on ALL data will be even larger.
;

_refine_ls_structure_factor_coef    Fsqd
_refine_ls_matrix_type              full
_refine_ls_weighting_scheme         calc

```

```

_refine_ls_weighting_details
'calc w=1/[\s^2^(Fo^2^)+(0.0284P)^2^+0.0000P] where P=(Fo^2^+2Fc^2^)/3'
_atom_sites_solution_primary      direct
_atom_sites_solution_secondary    difmap
_refine_ls_hydrogen_treatment     undef
_refine_ls_extinction_method      none
_refine_ls_extinction_coef        ?
_refine_ls_abs_structure_details
'Flack H D (1983), Acta Cryst. A39, 876-881'
_refine_ls_abs_structure_Flack    -0.15(7)
_refine_ls_number_reflns          1474
_refine_ls_number_parameters      92
_refine_ls_number_restraints      1
_refine_ls_R_factor_all           0.0514
_refine_ls_R_factor_gt            0.0338
_refine_ls_wR_factor_ref          0.0658
_refine_ls_wR_factor_gt          0.0625
_refine_ls_goodness_of_fit_ref    0.841
_refine_ls_restrained_S_all       0.841
_refine_ls_shift/su_max           0.000
_refine_ls_shift/su_mean          0.000

```

loop_

```

_atom_site_label
_atom_site_type_symbol
_atom_site_fract_x
_atom_site_fract_y
_atom_site_fract_z
_atom_site_U_iso_or_equiv
_atom_site_adp_type
_atom_site_occupancy
_atom_site_symmetry_multiplicity
_atom_site_calc_flag
_atom_site_refinement_flags
_atom_site_disorder_assembly
_atom_site_disorder_group
Na Na 0.0000 0.0000 0.0825(5) 0.0229(12) Uani 0.859(14) 6 d SP . .
YAL Al 0.12237(7) 0.06118(4) 0.50346(13) 0.0119(3) Uani 0.799(7) 2 d SP . .
YFE Fe 0.12237(7) 0.06118(4) 0.50346(13) 0.0119(3) Uani 0.201(7) 2 d SP . .
ZAL Al 0.29700(6) 0.36937(6) 1.14311(12) 0.0104(2) Uani 0.959(5) 1 d P . .
Si Si 0.19214(5) 0.19002(5) 0.86941(10) 0.0080(2) Uani 0.899(5) 1 d P . .
O1 O 0.0000 0.0000 0.6394(8) 0.0269(12) Uani 1 6 d S . .
O2 O 0.06060(11) 0.1212(2) 0.3556(4) 0.0210(7) Uani 1 2 d S . .
O3 O 0.2620(2) 0.13101(12) 0.3745(4) 0.0189(7) Uani 1 2 d S . .
O4 O 0.1869(2) 0.09346(11) 0.9640(4) 0.0198(6) Uani 1 2 d S . .
O5 O -0.1883(2) -0.09417(11) -0.0580(4) 0.0192(6) Uani 1 2 d S . .
O6 O 0.19549(14) 0.18438(14) 0.6403(3) 0.0150(4) Uani 1 1 d . . .
O7 O 0.28759(14) 0.28731(13) 0.9447(3) 0.0142(4) Uani 1 1 d . . .
O8 O 0.20909(14) 0.26975(14) 1.3046(3) 0.0145(4) Uani 1 1 d . . .
B B 0.10971(18) 0.2194(4) 0.3182(6) 0.0142(8) Uani 1 2 d S . .

```

loop_

```

_atom_site_aniso_label
_atom_site_aniso_U_11
_atom_site_aniso_U_22

```

```

_atom_site_aniso_U_33
_atom_site_aniso_U_23
_atom_site_aniso_U_13
_atom_site_aniso_U_12
Na 0.0223(15) 0.0223(15) 0.024(2) 0.000 0.000 0.0111(8)
YAL 0.0113(5) 0.0098(4) 0.0151(5) -0.00095(17) -0.0019(3) 0.0057(2)
YFE 0.0113(5) 0.0098(4) 0.0151(5) -0.00095(17) -0.0019(3) 0.0057(2)
ZAL 0.0113(4) 0.0109(4) 0.0098(4) -0.0004(3) 0.0001(3) 0.0060(3)
Si 0.0081(4) 0.0082(4) 0.0076(3) -0.0008(3) -0.0002(3) 0.0041(3)
O1 0.0314(19) 0.0314(19) 0.018(3) 0.000 0.000 0.0157(9)
O2 0.0251(13) 0.0147(14) 0.0197(14) 0.0002(12) 0.0001(6) 0.0073(7)
O3 0.0291(17) 0.0171(11) 0.0144(13) 0.0003(6) 0.0005(12) 0.0146(8)
O4 0.0243(16) 0.0168(10) 0.0208(14) 0.0000(6) -0.0001(12) 0.0121(8)
O5 0.0250(16) 0.0188(11) 0.0160(13) 0.0009(6) 0.0018(11) 0.0125(8)
O6 0.0165(10) 0.0169(10) 0.0111(8) 0.0008(7) 0.0012(7) 0.0080(8)
O7 0.0135(9) 0.0138(9) 0.0133(8) -0.0003(7) 0.0002(7) 0.0053(8)
O8 0.0136(9) 0.0152(10) 0.0153(9) 0.0018(7) -0.0001(7) 0.0075(8)
B 0.0172(16) 0.015(2) 0.0094(16) -0.0004(14) -0.0002(7) 0.0077(10)

```

```
_geom_special_details
```

```
;
```

All esds (except the esd in the dihedral angle between two l.s. planes) are estimated using the full covariance matrix. The cell esds are taken into account individually in the estimation of esds in distances, angles and torsion angles; correlations between esds in cell parameters are only used when they are defined by crystal symmetry. An approximate (isotropic) treatment of cell esds is used for estimating esds involving l.s. planes.

```
;
```

```
loop_
```

```

_geom_bond_atom_site_label_1
_geom_bond_atom_site_label_2
_geom_bond_distance
_geom_bond_site_symmetry_2
_geom_bond_publ_flag
Na O2 2.561(4) 3 y
Na O2 2.561(4) 2 y
Na O2 2.561(4) . y
Na O4 2.710(3) 1_554 y
Na O4 2.710(3) 2_554 y
Na O4 2.710(3) 3_554 y
Na O5 2.781(3) 3 y
Na O5 2.781(3) 2 y
Na O5 2.781(3) . y
YAL O2 1.981(2) . y
YAL O2 1.981(2) 3 y
YAL O6 1.965(2) 6 y
YAL O6 1.965(2) . y
YAL O1 1.944(3) . y
YAL O3 2.132(3) . y
ZAL O6 1.869(2) 15 y
ZAL O7 1.876(2) . y
ZAL O8 1.889(2) . y
ZAL O8 1.918(2) 15_554 y
ZAL O7 1.925(2) 8 y

```

ZAL O3 1.9890(15) 15 y
Si O7 1.625(2) . y
Si O5 1.6298(12) 3_556 y
Si O6 1.633(2) . y
Si O4 1.6412(15) . y
B O2 1.380(6) . y
B O8 1.373(3) 1_554 y
B O8 1.373(3) 5_554 y

_diffn_measured_fraction_theta_max	0.990
_diffn_reflns_theta_full	36.05
_diffn_measured_fraction_theta_full	0.990
_refine_diff_density_max	0.668
_refine_diff_density_min	-0.384
_refine_diff_density_rms	0.123

```

data_cemp_pr1

_audit_update_record
;
2010-12-22 # Formatted by publCIF
;

_audit_creation_method          SHELXL-97

_chemical_name_mineral         'oxy-schorl'
_chemical_compound_source      'Pibyslavice, Czech Republic'
_chemical_formula_sum
;
Al6.80 B3 Ca0.02 F0.31 Fe1.96 H3.11 K0.01
Mg0.19 Mn0.01 Na0.59 O30.69 Si5.94 Ti0.09
;
_chemical_formula_weight       1016.33

loop_
_atom_type_symbol
_atom_type_description
_atom_type_scatter_dispersion_real
_atom_type_scatter_dispersion_imag
_atom_type_scatter_source
'O' 'O' 0.0106 0.0060
'International Tables Vol C Tables 4.2.6.8 and 6.1.1.4'
'Na' 'Na' 0.0362 0.0249
'International Tables Vol C Tables 4.2.6.8 and 6.1.1.4'
'Fe' 'Fe' 0.3463 0.8444
'International Tables Vol C Tables 4.2.6.8 and 6.1.1.4'
'Al' 'Al' 0.0645 0.0514
'International Tables Vol C Tables 4.2.6.8 and 6.1.1.4'
'Si' 'Si' 0.0817 0.0704
'International Tables Vol C Tables 4.2.6.8 and 6.1.1.4'
'B' 'B' 0.0013 0.0007
'International Tables Vol C Tables 4.2.6.8 and 6.1.1.4'
'F' 'F' 0.0171 0.0103
'International Tables Vol C Tables 4.2.6.8 and 6.1.1.4'
'H' 'H' 0.0000 0.0000
'International Tables Vol C Tables 4.2.6.8 and 6.1.1.4'
'Ti' 'Ti' 0.2776 0.4457
'International Tables Vol C Tables 4.2.6.8 and 6.1.1.4'
'Mn' 'Mn' 0.3368 0.7283
'International Tables Vol C Tables 4.2.6.8 and 6.1.1.4'
'Mg' 'Mg' 0.0486 0.0363
'International Tables Vol C Tables 4.2.6.8 and 6.1.1.4'
'Ca' 'Ca' 0.2262 0.3064
'International Tables Vol C Tables 4.2.6.8 and 6.1.1.4'
'K' 'K' 0.2009 0.2494
'International Tables Vol C Tables 4.2.6.8 and 6.1.1.4'

_symmetry_cell_setting          trigonal
_symmetry_space_group_name_H-M  'R 3 m'

```

```

loop_
_symmetry_equiv_pos_as_xyz
'x, y, z'
'-y, x-y, z'
'-x+y, -x, z'
'-y, -x, z'
'-x+y, y, z'
'x, x-y, z'
'x+2/3, y+1/3, z+1/3'
'-y+2/3, x-y+1/3, z+1/3'
'-x+y+2/3, -x+1/3, z+1/3'
'-y+2/3, -x+1/3, z+1/3'
'-x+y+2/3, y+1/3, z+1/3'
'x+2/3, x-y+1/3, z+1/3'
'x+1/3, y+2/3, z+2/3'
'-y+1/3, x-y+2/3, z+2/3'
'-x+y+1/3, -x+2/3, z+2/3'
'-y+1/3, -x+2/3, z+2/3'
'-x+y+1/3, y+2/3, z+2/3'
'x+1/3, x-y+2/3, z+2/3'

_cell_length_a          15.9853(12)
_cell_length_b          15.9853(12)
_cell_length_c          7.1538(6)
_cell_angle_alpha      90.00
_cell_angle_beta       90.00
_cell_angle_gamma      120.00
_cell_volume            1583.1(2)
_cell_formula_units_Z   3
_cell_measurement_temperature 293(2)
_cell_measurement_reflns_used 2936
_cell_measurement_theta_min 2.8470
_cell_measurement_theta_max 36.0482

_exptl_crystal_description 'elongated grain'
_exptl_crystal_colour      'brown'
_exptl_crystal_size_max    0.30
_exptl_crystal_size_mid    0.10
_exptl_crystal_size_min    0.10
_exptl_crystal_density_meas ?
_exptl_crystal_density_diffn 3.198
_exptl_crystal_density_method 'not measured'
_exptl_crystal_F_000      1501
_exptl_absorpt_coefficient_mu 2.199
_exptl_absorpt_correction_T_min 0.80567
_exptl_absorpt_correction_T_max 1.00000
_exptl_absorpt_correction_type multi-scan
_exptl_absorpt_process_details
;
CrysAlis RED, Oxford Diffraction Ltd.,
Version 1.171.33.52 (release 06-11-2009 CrysAlis171 .NET)
(compiled Nov 6 2009,16:24:50)
Empirical absorption correction using spherical harmonics,
implemented in SCALE3 ABSPACK scaling algorithm.
;

```


_diffrn_ambient_temperature 293(2)
_diffrn_radiation_wavelength 0.71073
_diffrn_radiation_type MoK\alpha
_diffrn_radiation_source 'Enhance (Mo) X-ray Source'
_diffrn_radiation_monochromator graphite
_diffrn_measurement_device_type 'Kuma KM-4/Xcalibur-CCD(Sapphire2)'
_diffrn_measurement_method '\w scans'
_diffrn_detector_area_resol_mean 8.4353

_diffrn_reflns_number 4166
_diffrn_reflns_av_R_equivalents 0.0195
_diffrn_reflns_av_sigmaI/netI 0.0279
_diffrn_reflns_limit_h_min -26
_diffrn_reflns_limit_h_max 18
_diffrn_reflns_limit_k_min -25
_diffrn_reflns_limit_k_max 23
_diffrn_reflns_limit_l_min -8
_diffrn_reflns_limit_l_max 11
_diffrn_reflns_theta_min 3.21
_diffrn_reflns_theta_max 36.07
_reflns_number_total 1380
_reflns_number_gt 1285
_reflns_threshold_expression >2sigma(I)

_computing_data_collection

;
CrysAlis CCD, Oxford Diffraction Ltd.,
Version 1.171.33.52

;
_computing_cell_refinement

;
CrysAlis RED, Oxford Diffraction Ltd.,
Version 1.171.33.52

;
_computing_data_reduction

;
CrysAlis RED, Oxford Diffraction Ltd.,
Version 1.171.33.52

;
_computing_structure_solution 'SHELXS-97 (Sheldrick, 2008)'
_computing_structure_refinement 'SHELXL-97 (Sheldrick, 2008)'
_computing_publication_material 'SHELXL-97 (Sheldrick, 2008)'

_refine_special_details

;
Refinement of F^2 against ALL reflections. The weighted R-factor wR and goodness of fit S are based on F^2 , conventional R-factors R are based on F , with F set to zero for negative F^2 . The threshold expression of $F^2 > 2\sigma(F^2)$ is used only for calculating R-factors(gt) etc. and is not relevant to the choice of reflections for refinement. R-factors based on F^2 are statistically about twice as large as those based on F , and R-

factors based on ALL data will be even larger.

;

```
_refine_ls_structure_factor_coef Fsqd
_refine_ls_matrix_type full
_refine_ls_weighting_scheme calc
_refine_ls_weighting_details
'calc w=1/[\s^2^(Fo^2^)+(0.0207P)^2^+0.0000P] where P=(Fo^2^+2Fc^2^)/3'
_atom_sites_solution_primary direct
_atom_sites_solution_secondary difmap
_atom_sites_solution_hydrogens geom
_refine_ls_hydrogen_treatment reffall
_refine_ls_extinction_method SHELXL
_refine_ls_extinction_coef 0.00058(10)
_refine_ls_extinction_expression
'Fc^^=kFc[1+0.001xFc^2^\l^3^/sin(2\q)]^-1/4^'
_refine_ls_abs_structure_details
'Flack H D (1983), Acta Cryst. A39, 876-881'
_refine_ls_abs_structure_Flack 0.005(16)
_refine_ls_number_reflns 1380
_refine_ls_number_parameters 96
_refine_ls_number_restraints 1
_refine_ls_R_factor_all 0.0211
_refine_ls_R_factor_gt 0.0191
_refine_ls_wR_factor_ref 0.0401
_refine_ls_wR_factor_gt 0.0398
_refine_ls_goodness_of_fit_ref 0.976
_refine_ls_restrained_S_all 0.976
_refine_ls_shift/su_max 0.001
_refine_ls_shift/su_mean 0.000
```

loop_

```
_atom_site_label
_atom_site_type_symbol
_atom_site_fract_x
_atom_site_fract_y
_atom_site_fract_z
_atom_site_U_iso_or_equiv
_atom_site_adp_type
_atom_site_occupancy
_atom_site_symmetry_multiplicity
_atom_site_calc_flag
_atom_site_refinement_flags
_atom_site_disorder_assembly
_atom_site_disorder_group
Na Na 0.0000 0.0000 0.9019(5) 0.0266(11) Uani 0.676(10) 6 d SP . .
YFE Fe 0.87496(3) 0.937481(16) 0.50264(6) 0.00869(12) Uani 0.621(4) 2 d SP . .
YAL Al 0.87496(3) 0.937481(16) 0.50264(6) 0.00869(12) Uani 0.379(4) 2 d SP . .
ZAL Al 0.70355(3) 0.63191(3) -0.14783(6) 0.00590(13) Uani 0.974(3) 1 d P . .
ZFE Fe 0.70355(3) 0.63191(3) -0.14783(6) 0.00590(13) Uani 0.026(3) 1 d P . .
Si Si 0.80806(3) 0.81008(3) 0.12963(6) 0.00569(10) Uani 1 1 d . . .
O1 O 0.0000 0.0000 0.3485(5) 0.0363(9) Uani 0.69 6 d SP . .
F F 0.0000 0.0000 0.3485(5) 0.0363(9) Uani 0.31 6 d SP . .
O2 O 0.93822(6) 0.87643(12) 0.6435(3) 0.0151(4) Uani 1 2 d S . .
O3 O 0.73144(14) 0.86572(7) 0.6201(2) 0.0123(3) Uani 1 2 d S . .
```

O4 O 0.81267(12) 0.90634(6) 0.0387(2) 0.0103(3) Uani 1 2 d S . .
O5 O 0.18631(12) 0.09316(6) 0.0618(2) 0.0104(3) Uani 1 2 d S . .
O6 O 0.80182(8) 0.81238(8) 0.35415(17) 0.0089(2) Uani 1 1 d . . .
O7 O 0.71481(8) 0.71419(8) 0.05039(16) 0.0086(2) Uani 1 1 d . . .
O8 O 0.79017(8) 0.72936(8) -0.31139(16) 0.0097(2) Uani 1 1 d . . .
B B 0.88991(10) 0.77981(19) 0.6753(4) 0.0076(4) Uani 1 2 d S . .
H3 H 0.735(2) 0.8677(12) 0.732(5) 0.021(8) Uiso 1 2 d S . .

loop_

_atom_site_aniso_label
_atom_site_aniso_U_11
_atom_site_aniso_U_22
_atom_site_aniso_U_33
_atom_site_aniso_U_23
_atom_site_aniso_U_13
_atom_site_aniso_U_12
Na 0.0267(13) 0.0267(13) 0.0263(18) 0.000 0.000 0.0134(7)
YFE 0.0087(2) 0.00611(15) 0.0121(2) -0.00108(7) -0.00216(15) 0.00433(10)
YAL 0.0087(2) 0.00611(15) 0.0121(2) -0.00108(7) -0.00216(15) 0.00433(10)
ZAL 0.0062(2) 0.0058(2) 0.0058(2) -0.00008(16) 0.00034(15) 0.00309(18)
ZFE 0.0062(2) 0.0058(2) 0.0058(2) -0.00008(16) 0.00034(15) 0.00309(18)
Si 0.0054(2) 0.00520(19) 0.0064(2) -0.00044(14) -0.00021(15) 0.00266(15)
O1 0.0494(15) 0.0494(15) 0.0102(15) 0.000 0.000 0.0247(8)
F 0.0494(15) 0.0494(15) 0.0102(15) 0.000 0.000 0.0247(8)
O2 0.0207(7) 0.0069(7) 0.0132(8) 0.0008(6) 0.0004(3) 0.0035(4)
O3 0.0213(9) 0.0123(6) 0.0063(7) 0.0004(3) 0.0007(6) 0.0107(4)
O4 0.0145(8) 0.0074(5) 0.0114(8) 0.0006(3) 0.0011(6) 0.0072(4)
O5 0.0149(8) 0.0082(5) 0.0105(7) 0.0006(3) 0.0012(6) 0.0075(4)
O6 0.0090(5) 0.0103(5) 0.0070(5) -0.0009(4) -0.0003(4) 0.0047(4)
O7 0.0088(5) 0.0068(5) 0.0082(5) -0.0008(4) -0.0009(4) 0.0024(4)
O8 0.0075(5) 0.0115(5) 0.0111(5) 0.0021(4) 0.0010(4) 0.0054(5)
B 0.0077(7) 0.0074(10) 0.0074(10) 0.0000(8) 0.0000(4) 0.0037(5)

_geom_special_details

;
All e.s.d.'s (except the e.s.d. in the dihedral angle between two l.s. planes) are estimated using the full covariance matrix. The cell e.s.d.'s are taken into account individually in the estimation of e.s.d.'s in distances, angles and torsion angles; correlations between e.s.d.'s in cell parameters are only used when they are defined by crystal symmetry. An approximate (isotropic) treatment of cell e.s.d.'s is used for estimating e.s.d.'s involving l.s. planes.

;

loop_

_geom_bond_atom_site_label_1
_geom_bond_atom_site_label_2
_geom_bond_distance
_geom_bond_site_symmetry_2
_geom_bond_publ_flag
Na O2 2.519(3) 1_445 y
Na O2 2.519(3) 3_565 y
Na O2 2.519(3) 2_655 y
Na O4 2.772(2) 3_566 y
Na O4 2.772(2) 1_446 y

Na O4 2.772(2) 2_656 y
Na O5 2.821(2) 2_556 y
Na O5 2.821(2) 1_556 y
Na O5 2.821(2) 3_556 y
YFE O2 1.9941(12) . y
YFE O2 1.9942(12) 3_675 y
YFE O6 2.0387(13) 6_565 y
YFE O6 2.0387(13) . y
YFE O1 2.052(2) 1_665 y
YFE O3 2.1572(19) . y
ZAL O6 1.8615(13) 9_564 y
ZAL O7 1.8804(12) . y
ZAL O8 1.8857(12) . y
ZAL O8 1.9264(12) 9_565 y
ZAL O7 1.9589(12) 14_654 y
ZAL O3 1.9814(9) 9_564 y
Si O6 1.6108(13) . y
Si O7 1.6149(11) . y
Si O5 1.6253(7) 3_665 y
Si O4 1.6380(8) . y
B O2 1.357(3) . y
B O8 1.3841(18) 1_556 y
B O8 1.3841(18) 5_656 y

_diffn_measured_fraction_theta_max 0.990
_diffn_refl_theta_full 36.07
_diffn_measured_fraction_theta_full 0.990
_refine_diff_density_max 0.652
_refine_diff_density_min -0.495
_refine_diff_density_rms 0.083